AN UPSCALING TECHNIQUE FOR HETEROGENEOUS POROUS MEDIA BASED ON A FINITE DIFFERENCE SOLUTION FOR THE DIFFUSIVITY EQUATION

Andrea Failla

andrea1.failla@mail.polimi.it

Politecnico Di Milano

Facoltà di Ingegneria Industriale, Milano, Italy

Luiz Adolfo Hegele Jr.

Lindaura Maria Steffens

luiz.hegele@udesc.br

lindaura.steffens@udesc.br

Universidade do Estado de Santa Catarina-UDESC

CESFI, Av. Central, 413, 88330-668, Balneário Camboriú, Santa Catarina, Brasil

Abstract. *In this work a numerical upscaling technique for absolute permeability and single-phase flow based on the finite-difference method is developed. The new method has firstly been applied to artificial grids. In particular, symmetric and stratified meshes were used in order to compare analytical results with the ones obtained from the new technique. Then, the method was applied to two SPE's dataset and some permeability fields generated by numerical probability distribution. A large number of simulations wells were done in order to compare well flows of both fine and coarse models. The results in terms of well flow comparison can be considered satisfactory, especially when the production well is located in a high permeability zone of the reservoir.*

Keywords: *Upscaling techniques, Absolute Permeability, Single-Phase Flow, Reservoir Simulation, Finite-Difference Method.*

1 INTRODUCTION

The main objective of reservoir flow simulations is to obtain the flow field involved in hydrocarbon recovery to enable prediction of production volumes. These aims require numerical modelling of the mathematics and physics of the flow processes including mass balance and Darcy's law.

A geological model is required where the reservoir is described as a mesh of grid cells. The model requires input parameters such as a permeability and porosity distribution, relative permeability functions, etc. Through advanced instruments, methods and measurements, is possible to obtain a good knowledge about hydrocarbons deposits and to make accurate three-dimensional geological models. The data are obtained on a different scale, generally lower, than that used to discretize the numerical reservoir model. So many flow simulators cannot deal directly and effectively with the size of the mesh used in geological models. Nowadays, these models can be consist of 10 million active cells, while the simulations can be performed within a reasonable time with models of the order of hundreds of cells (Christie, 1996). Unfortunately, it is impossible to run fluid flow simulations in a reasonable computational time in complicated geological models. In fact, software for flow simulations are still limited.

Therefore, an important issue in the numerical simulation of flow in reservoirs is the scale problem. Accurate representation of the geology requires some form of averaging of parameters. Thus, the upscaling concept arises, which is a process of obtaining a coarse mesh (low resolution - discretization scale), which is better suited to the simulation based on fine mesh (high resolution – measurement scale). This implies a model for achieving results through simulations preserving the representative behavior, even omitting much of the fine detail of the geological model. Therefore, upscaling techniques on rock properties are used for the reduction of the geological scale, allowing production/injection flow simulations.

The upscaling process determines the effective property value of a heterogeneous model represented by a correspondent homogeneous model (Odsaeter, 2013). In this way, is possible to run fluid flow simulations with reasonable time consumption. Upscaling a fine geological model is always a fundamental and critical step in reservoir simulation processes. In other words, it is essentially an averaging procedure where those of the coarse one, as illustrated in Fig. 1, approximate the static and dynamic characteristics of the fine scale model.

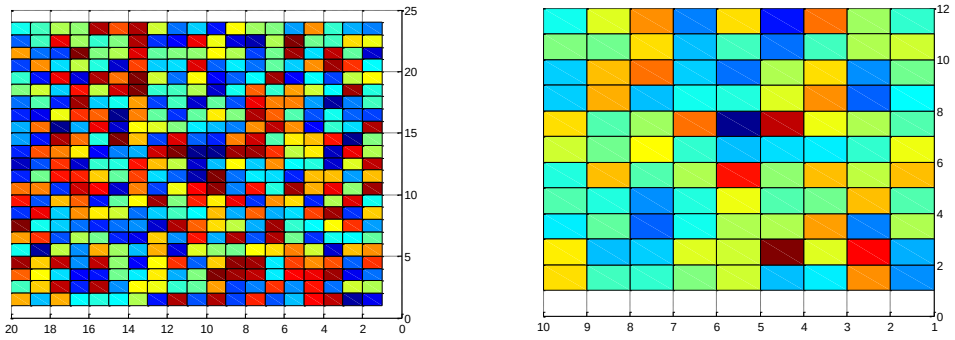

Figure 1. Example of upscaling field. The fine model (on the left) and the scaled up (on the right) obtained by applying harmonic average technique

The process that precedes the upscaling is called homogenization. It consists in setting one single value of a given property for the heterogeneous region to be upscaled. Upscaling techniques are nowadays so important and cannot be avoided. However, replacing a more detailed model with an approximated one implies the loss of several informations. The direct consequence is a lower quality prediction of flow rates and pressure distributions.

The techniques for upscaling from the simple calculation averaging for the heterogeneous values within block to sophisticated inversions. The simple and combined averages methods are easy to implement and are still technical standard estimates in the oil industry, even though for many the simple average distributions are not good estimates. For example, the geometric average of a finite fraction distribution with zero permeability is zero, even though the system may have a total permeability nonzero. To overcome this difficulty, several attempts have been made. Harmonic and arithmetic average techniques are used in different cases. In fact, their application depends on the main permeability change direction. Whereas, power average includes a parameter (p) which depends on the permeability distribution. Besides, for additive properties, it is easy to achieve a good approximation of the original fine grid. Volumetric (or additive) properties, such as porosity and saturation, do not need particular scaling technique. Their upscaled representation is given by simple averaging methods. However, when dealing with non-additive properties, such as the absolute permeability, it is not always possible to approximate effective values by simply using weighted arithmetic average techniques. In fact, in this case the problem is complicated, it is necessary to take into account different aspects.

A great number of works in thesis and papers have been published on this subject in the last years (White and Horne (1987), Kruel-Romeu (1994), Wen et al. (2003), Odsaeter (2013)). Wen and Gómez-Hernández (1996) and Renard and Marsily (2000), present a detailed review of the main methods and procedures of the upscaling, describing its advantages and limitations.

In this work, we describe a new numerical upscaling technique for absolute permeability based on single-phase flow and the finite-difference method.

2 PROBLEM STATEMENT

2.1 Basic Equation for Single-Phase Flow

The most famous law used in reservoir simulation to describe flow in porous media is Darcy's law, considering the following assumptions: laminar and single-phase flow, Newtonian and homogeneous fluids, no chemical and kinetic interactions between the fluid and the rock. The Darcy's law is an empirical relationship between fluid flow rate and gradient of pressure (or hydraulic gradient). Mathematically, for single-phase flow, defined as:

$$q = -\frac{\mathbf{k}}{\mu}\left(\overrightarrow{\nabla p} - \rho g\right)A, \tag{1}$$

where μ is the fluid viscosity, $\overrightarrow{\nabla p}$ is the gradient of pressure, ρg is the gravitational term, A is the cross-sectional area and $\mathbf{k}$ is the absolute rock permeability tensor, mathematically represented by:

$$\mathbf{k} = \begin{bmatrix} k_{xx} & k_{yx} & k_{xz} \\ k_{yx} & k_{yy} & k_{yz} \\ k_{zx} & k_{zy} & k_{zz} \end{bmatrix}. \tag{2}$$

The absolute permeability tensor is an intrinsic property of the porous medium. Thus, it does not depend on pressure, temperature or the fluid flow. Assuming that the coordinate system and the principal axes of the permeability tensor are aligned, results in a diagonalized permeability tensor:

$$\mathbf{k} = \begin{bmatrix} k_{xx} & 0 & 0 \\ 0 & k_{yy} & 0 \\ 0 & 0 & k_{zz} \end{bmatrix}. \tag{3}$$

It is noteworthy that the absolute permeability tensor is defined for each grid-block. Thus, if the cells are isotropic, becomes $k_{xx} = k_{yy} = k_{zz}$. This is a further simplification of the analysis, valid only for the fine model, because it is commonly discretized to have homogeneous cells.

The basic equation to describe the flow in porous media caused by a potential difference is known as the **diffusivity equation**. The diffusivity equation is derived from three physical principles: conservation of mass, conservation of momentum (Darcy's Law) and an equation of state. Thus, deriving the diffusivity equation for single-phase flow we obtains

$$\nabla \cdot \left(\frac{A\mathbf{k}}{\mu B} \nabla p \right) = \frac{\partial}{\partial t} \left(\frac{\phi}{B} \right) + \tilde{q}, \tag{4}$$

where ϕ is the porosity, B is fluid volume factor and $\tilde{q}$ is the source term. Assuming slightly compressible fluid and there is no source term the Eq. (4) yields

$$\nabla \cdot (\mathrm{A}\mathbf{k} \nabla p) = 0. \tag{5}$$

2.2 Finite-Difference Approximation

The flow equations can be converted to a numerical model by discretization of the porous medium into a finite number of cells. The most common numerical methods used in oil industry are based on the finite-difference method (Fitts, 2002). The purpose of a grid system is to assign to each cell their own values of rock properties, pressure and temperature. The diffusivity equation contain continuous derivatives of second order in space and first order in time. Due to their non-linear nature, it is impossible to solve them using any analytical approach. Discretization processes help reservoir engineers for overcoming this obstacle.

Spatial Approximation: The discretization in space can be performed by blocks that store their property in its center as shown in Fig. 2.

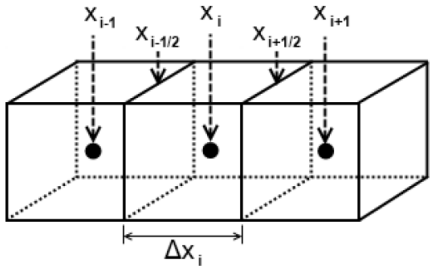

Figure 2. Example grid notation for one-dimensional space discretization

For rectangular or square geometries, namely Cartesian coordinates, the grid-points are defined as the grid-blocks centre. The Eq. (4), diffusivity equation, in Cartesian coordinates system can be written as

$$\underbrace{\frac{\partial}{\partial x}\left(\frac{A_x k_x}{\mu B}\frac{\partial p}{\partial x}\right)}_{S_x} + \underbrace{\frac{\partial}{\partial y}\left(\frac{A_y k_y}{\mu B}\frac{\partial p}{\partial y}\right)}_{S_y} + \underbrace{\frac{\partial}{\partial z}\left(\frac{A_z k_z}{\mu B}\frac{\partial p}{\partial z}\right)}_{S_z} = \underbrace{\frac{\partial}{\partial t}\left(\frac{\phi}{B}\right)}_{S_t} + \underbrace{\tilde{q}}_{S_q} \tag{6}$$

Using the central-difference approximations for the first order derivatives, the spatial discretization for the term on the left side of Eq. (6), that is, the partial derivative in x-direction, can be written as

$$S_x = \frac{\partial}{\partial x}\left(\frac{A_x k_x}{\mu B}\frac{\partial p}{\partial x}\right)_i \cong \frac{1}{\Delta x_i}\left[\left(\frac{A_x k_x}{\mu B}\frac{\partial p}{\partial x}\right)_{i+\frac{1}{2}} - \left(\frac{A_x k_x}{\mu B}\frac{\partial p}{\partial x}\right)_{i-\frac{1}{2}}\right] \tag{7}$$

as also using the central-difference to the first derivative of the pressure, given as

$$\left(\frac{\partial p}{\partial x}\right)_{i\pm\frac{1}{2}} = \pm\frac{p_{i\pm1} - p_i}{\Delta x_{i\pm\frac{1}{2}}}. \tag{8}$$

Thus, the first term of left side of Eq. (6), results as

$$S_x = \frac{\partial}{\partial x}\left(\frac{A_x k_x}{\mu B}\frac{\partial p}{\partial x}\right)_i \cong \frac{1}{\Delta x_i}\left[\left(\frac{A_x k_x}{\mu B \Delta x}\right)_{i+\frac{1}{2}}(p_{i+1} - p_i) - \left(\frac{A_x k_x}{\mu B \Delta x}\right)_{i-\frac{1}{2}}(p_i - p_{i-1})\right], \tag{9}$$

such that, results the transmissibility property definition, expressed as

$$T_{x_{i\pm\frac{1}{2}}} = \left(\frac{A_x k_x}{\mu B \Delta x}\right)_{i\pm\frac{1}{2}}. \tag{10}$$

This property depends on porous medium and due to the fact that block-centered grids, the transmissibility coefficient must be evaluated on the block's boundaries. It means that permeability will be given by the harmonic mean between two cells connected in series, that is:

$$(k_x)_{i+\frac{1}{2}} = \frac{n}{\sum_{i=1}^{n} \frac{1}{k_i}}. \tag{11}$$

Therefore, we obtain

$$S_x \cong \frac{1}{\Delta x_i}\left[T_{x_{i+\frac{1}{2}}}(p_{i+1} - p_i) - T_{x_{i-\frac{1}{2}}}(p_i - p_{i-1})\right], \tag{12}$$

Similarly for the partial derivatives in y and z, we obtain the spatial discretization for the terms S_y and S_z, respectively.

Time Approximation: There are two methods for the discretization of differential equations dependent of the time, namely: explicit and implicit methods. The BTCS implicit method (backward-time, central-space) to approximate the partial derivative of the first order in time for a backward finite-difference is unconditionally stable (Chen, 2007). For this reason, we will use the backward finite-difference to discretize the time coordinate. Therefore, backward finite-difference for the time derivative, the right slide of Eq. (6) gives

$$S_t^{n+1} \cong \frac{\gamma^{n+1}}{\Delta t}(p^{n+1} - p^n), \tag{13}$$

with

$$\gamma^{n+1} = \frac{\partial}{\partial p}\left(\frac{\phi}{B}\right),$$

where the index n represents the iteration at time t_n, Δt the step time and γ assumes different values, depending of the compressibility fluid assumption (compressible, slightly compressible or incompressible).

Thus, the discretization form of the diffusivity equation in one-dimensional can be written in the simplified way as

$$L_i p_{i+1}^{n+1} + M_i p_i^{n+1} + N_i p_{i-1}^{n+1} = C_i \text{ w}, \tag{14}$$

such that

$$L_i = T_{x_{i+\frac{1}{2}}}^{n+1},$$

$$N_i = T_{x_{i+\frac{1}{2}}}^{n+1},$$

$$M_i = -(\gamma_i^{n+1} + L_i + N_i),$$

$$C_i = -\left(\frac{\gamma_i^{n+1}}{\Delta t} p_i^n\right) + \tilde{q}_{lsci}^n,$$

where the subscript *l* indicates a single-phase fluid flow (oil or water). Similarly, we can obtain the simplified form for two and three dimensions, including the terms related to *j* and *k*, with the necessary algebraic manipulations. The term on the left hand side of Eq. (14) is the amount

of fluid that flows at time $(n+1)$, from a block to another one, whereas the term on the right side is the fluid accumulation for the block i.

3 THE NUMERICAL UPSCALING METHOD

The method proposed in this paper is based on the flow rate conservation. Every single cell which belongs to the fine grid will be considered homogeneous and isotropic.

A set of cells at the fine grid is chosen as the cells to be upscaled for the coarse grid. The pressure field is then solved for the fine grid, and then flow rates are calculated.

For the sake of simplicity, without losing generality, we will proceed with the explanation of the method for two dimensions. The grid shown in Fig. 3 is a piece of the heterogeneous medium to be upscaled. The homogenization process will be applied on the region made up of blocks 3, 4, 5 and 6 – from now on called *upscaling zone*, originally characterized by permeabilities k_3, k_4, k_5 and k_6, respectively. Two different sets of boundary conditions will be used in order to calculate the coarse grid, resulting in two equivalent permeabilities: $k_{eq,x}$ and $k_{eq,y}$. For the first set of boundary conditions, no-flow condition is applied at the boundaries located on the north and south of the fine grid region, and prescribed different pressures are applied on the left and right boundaries of the fine grid. Once this system is numerically solved, the total flow in the x direction, named q_x, is known.

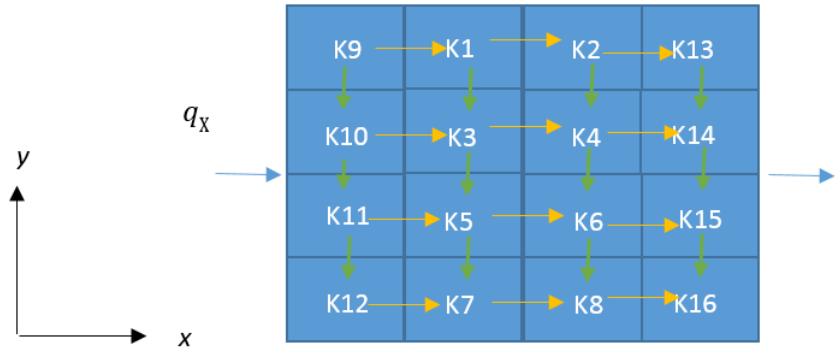

Figure 3. Region of the fine grid to be upscaled, with permeabilities K3, K4, K5 and K6. For the first run, no-flow condition is applied at the boundaries located on the north and south of the fine grid region, and different prescribed pressures are applied at the left and right boundaries.

For the second set of boundary conditions, shown in Fig. 4, now the no-flow condition is applied at the east and west boundaries, whilst the prescribed pressures are now applied on the north and south, giving rise to the flow in the y-direction, q_y.

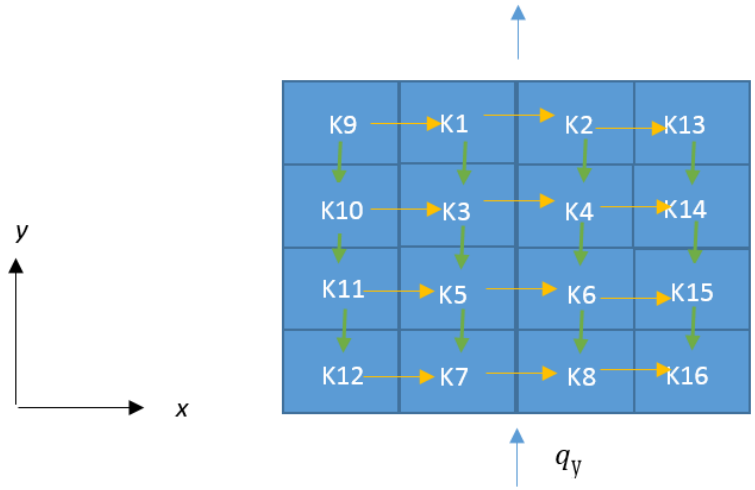

Figure 4. Region of the fine grid to be upscaled, with permeabilities K3, K4, K5 and K6. For the second run, no-flow condition is applied at the boundaries located on the west and east of the fine grid region, and different prescribed pressures are applied at the north and south boundaries.

The cells around the *upscaling zone* influence the equivalent permeability, reducing the influence of the boundary conditions. The cell layer around the *upscaling zone* will be called *ring*. Note that the ring exhibited in Figs. 3 and 4 is only one volume wide. It is possible to consider a wider *ring*, but this option will not be explored here.

With the value of q_x and q_y at hand, it is now possible to proceed with the homogenization process. The value of the flow rate for the x-direction is given by:

$$q_x \approx \left(p_2^{(1,x)} - p_1^{(1,x)}\right)k_{1,2} + \left(p_4^{(1,x)} - p_3^{(1.x)}\right)k_{3,4} + \left(p_6^{(1,x)} - p_5^{(1,x)}\right)k_{5,6} + \left(p_8^{(1,x)} - p_7^{(1,x)}\right)k_{7,8},$$

where $k_{i,j}$ refers to the harmonic mean between the permeabilities k_i and k_j, and the superscript *(1,x)* refers to the first run in the *x*-direction. The same applies for the y-direction,

$$q_y \approx \left(p_{10}^{(1,y)} - p_{11}^{(1,y)}\right)k_{10,11} + \left(p_3^{(1,y)} - p_5^{(1,y)}\right)k_{3,5} + \left(p_4^{(1,y)} - p_6^{(1,y)}\right)k_{4,6} + \left(p_{14}^{(1,y)} - p_{15}^{(1,y)}\right)k_{14,15}.$$

Our aim is to substitute $k_{3,4}$ and $k_{5,6}$ by $k_{eq,x}$, resulting in the first approximation for the equivalent permeability in the *x*-direction:

$$k_{eq,x}^{(1)} \approx \frac{q_x - \left(p_2^{(1,x)} - p_1^{(1,x)}\right)k_{1,2} - \left(p_8^{(1,x)} - p_7^{(1,x)}\right)k_{7,8}}{\left(p_4^{(1,x)} - p_3^{(1,x)}\right) + \left(p_6^{(1,x)} - p_5^{(1,x)}\right)}.$$

It can be seen that the equivalent permeability $k_{eq,x}^{(1)}$ will not, in general, lead to the same solution for the set of pressures $p_i^{(1,x)}$. Hence, the flow rate q_x also will not be retrieved with this initial guess for the equivalent permeability. This will result in a coupled non-linear system, since the same applies to the y-direction.

Numerical methods based on iterative cycles may present some convergence and stability problems. However, achieving the convergence can depend on the first trial values that have to be chosen or calculated. Due to the fact that the pressure distribution and the equivalent permeability vary proportionally, for each system, it could theoretically be possible to choose indifferently an initial best guess. In practice, it could be cumbersome to start the iterative process choosing a single pressure value as a first try. It makes more sense calculate a first try of equivalent permeability, and this is done using the permeability values by simply using the original pressure distribution.

In other words, the coefficient matrix for the systems –*x* and *y* directions - varies due to the introduction of equivalent permeabilities, and as a consequence also the pressure distributions vary. The set of flow equations that is used to calculate the pressure distribution is non-linear, and we have implemented an iterative process in order to solve this non-linear set of equations. The solution of this set of equations will result in the homogenized grid pictured in Fig. 5.

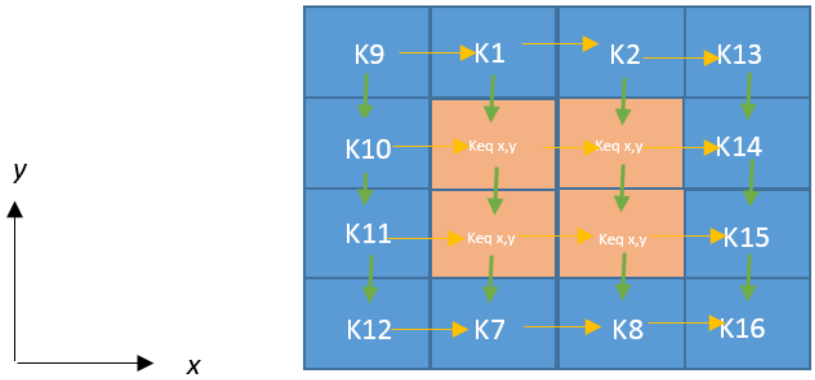

Figure 5. Upscaled region; the flow rates q_x and q_y are kept constant.

The final result will exhibit equivalent – and generally different – permeabilities in *x* and *y* directions, and this is the main feature of this technique: less cells to evaluate with a possibly higher degree of anisotropy.

4 NUMERICAL RESULTS

Firstly, the strategy to assess the numerical upscaling method of the permeability presented in the previous sections is validated for a log-normal permeability distribution randomly generated. Moreover, the performance of the upscaling method is analyzed for two different SPE's datasets, available on the SPE's website. The efficiency of the method is analyzed by comparing the well flows (production rates) in the fine and coarse meshes, respectively, as well as the simulation time. In addition, the influence of the use *rings* around

of the core to be homogenized, regions with low permeability and heterogeneity of the models are also discussed.

The error analyses in all cases is calculated as

$$E_p = \left| \frac{q_{fine} - q_{coarse}}{q_{fine}} \right| \tag{15}$$

where q_{fine} and q_{coarse} are the well flow in the fine and coarse meshes, respectively.

The role of surrounding blocks is to reduce the influence of the boundary conditions. We have performed several simulations, not shown in the present work, and we have not seen significant differences on the final results using more rings around the core. Therefore, we have used for all simulations only one *ring*, namely one block layer around the core.

Log-normal distribution: is the most appropriate in order to describe a permeability field. Therefore, the first model studied is a square two-dimension matrix (60x60) with a log-normal probability distribution of the permeability. Well production results generated and obtained are shown in the Table 1.

Table 1. Well production results for wells placed in different cells for a log-normal distribution of permeability generated in a 2D model.

Log-normal Distribution – 2D Model					
Fine Model		Coarse Model (resolution 2x2)			
κ	q_{fine}	$\kappa_{eq,x}$	$\kappa_{eq,y}$	q_{coarse}	$E_p(\%)$
1,19	3,51	0,57	0,52	3,59	2%
1,42	4,3	0,97	0,96	4,31	0%
0,55	3,13	0,59	0,62	4,01	28%
1,66	3,93	0,61	0,74	3,94	0%
0,81	3,87	0,65	0,92	4,47	15%
1,06	4,07	0,91	0,8	4,44	9%
0,55	3,09	0,79	0,9	4,18	35%

The wells were placed in different cells mesh. The well-cell permeability and the well-flow (fine mesh) are indicated in the first and second column, respectively. Results obtained using the numerical upscaling method, described in Section 3, corresponding the equivalent permeabilities (*x*- and *y*- main directions) and its well-flow (coarse mesh) are presented in the third to fifth columns. Finally, the last column presents the error, defined by Eq. (15), providing the difference the flow gap between the meshes. Noting that, the coarse mesh two-dimension

matrix (30x30 -resolution 2x2) is given by a fourth the fine mesh cells, that is, for each four cells with different permeabilities the upscaling process obtained an equivalent permeability transformed into a single cell. In this example, the fine mesh has 3600 cells, while the coarse mesh has only 900 cells.

The analysis of the results of Table 1 reveals that the estimate of the well-flow q_{coarse} obtained by upscaling method yields very good approximation of the q_{fine} in most cases. However, note that the when wells are placed in cells with low permeability or when the permeability in the main directions differs substantially (larger heterogeneity) in the coarse mesh the errors increase.

SPE's Datasets

The next two models are used to analyze the proposed upscaling method. These models were obtained from SPE Comparative Solution Project (SPE, 2001). The datasets was developed as a benchmark to compare the performance of different methods or algorithms held in Houston, Texas, in February of 2001. In particular, interest was placed in studying the behavior of upscaling and upgridding algorithms for the computation of the permeability fields. In the other words, the aim of these datasets is to compare differents tecniques and its abilities to predict performance of a geological model.

SPE dataset 1: is a two-phase (oil and gas) and the computational domain is a vertical cross-section without dipping and faults. The dimension of the model are $\Delta x = 7{,}62m;\ \Delta y = 7{,}62m$ and$\Delta z = 0{,}762m$. The fine scale grid *100* x*1* x*20* with uniform size for each of the grid blocks. In the present work, the mono-phase model with incompressible and immiscible fluid has to be considered and the permeability distribution is a correlated geostastically generated field with constant porosity $\phi = 0{,}2$. For simplification purposes, variables such as viscosity, density and saturation are considered as 1.

The computational time is very important in reservoir studies, as well as the difference between the production rates calculated using the fine and coarse grids. Some results of the simulation time, i.e., time consumed for the matrix inversion, for the model described by SPE dataset 1 are shown in the Table 2.

Table 2. Results of simulation time for the SPE's dataset 1

SPE dataset 1 - Simulation Time				
Fine Model		Coarse Model		
Dimension	Time [s]	Dimension	Resolution	Time [s]
100x20	2,05	50x10	2x2	0,07
100x20	2,22	25x5	4x4	0,019

It can be seen from the results that the upscaling process reduces computational time about 30 times for the 2x2 resolution, and more than 100 times for the 4x4 resolution case.

Analogous to log-normal distribution, well production results for this case are shown in the Table 3. Again, the wells were placed in different cells mesh. The well-cell permeability and the well-flow (fine mesh) are indicated in the first and second column, respectively. Results obtained using the numerical upscaling method, corresponding the equivalent permeabilities (*x*- and *y*- main directions) and its well-flow (coarse mesh) are presented in the third to fifth columns. The last column presents the error.

Table 3. Results of production well flows, using the SPE's dataset number 1

SPE dataset 1 – Well Production					
Fine Model		Coarse Model (resolution 2x2)			
κ	q_{fine}	$\kappa_{eq,x}$	$\kappa_{eq,y}$	q_{coarse}	$E_p(\%)$
78,45	14,62	66,90	67,47	14,85	1%
7,69	9,91	1,46	2,93	7,52	24%
321,87	11,06	20,67	20,12	11,74	6%
11,12	12,11	89,17	112,96	15,61	28%
20,34	13,27	38,86	39,26	15,00	12%

Note that, the results of Table 3 reveals that the estimate of the well-flow obtained by upscaling method yields very good approximation, especially for high values of permeability.

SPE dataset 2-2D: the computational model has a simple rectangular geometry without top structure or faults. The fine geological model scale is described on a regular Cartesian mesh with dimensions $\Delta x = 1200ft$, $\Delta y = 2200ft$ and $\Delta z = 170ft$. The reservoir description consists of a Brent sequence, where the top part is a Tarbert formation (prograding near shore environment) and the lower part is a Upper Ness (fluvial) (SPE, 2001). The fine scale cell size is 20ft x 10ft x 2ft which corresponds the cells number 60x220x84. As *SPE dataset 2* contains a great number of elements, to simulate it in two dimensions only its top layer has been taken into account. The fine model size was *60*x*84*. The results of simulation time for the model described by SPE dataset 2 are shown in Table 3.

Table 3. Results of simulation time for the SPE's dataset 2

SPE dataset 2 - Simulation Time				
Fine Model		Coarse Model		
Dimension	Time [s]	Dimension	Resolution	Time [s]
60x84	24,33	30x42	2x2	0,811
60x84	24,27	15x21	4x4	0,044
60x84	24,27	10x14	6x6	0,018

Once more, the second and fifth columns show the times for both, fine and coarse grids, respectively. Note that the use of coarse grid for simulation provides a larger reduction of the time: 30 times for the 2x2 resolution, more than 500 times for the 4x4 resolution and about 1300 times for the last case (6x6 resolution).

Analogous to the previous cases, well production results for this setup are shown in the Table 4.

Table 4. Results of production well flows, using the SPE's dataset number 2

SPE dataset 2 - Well Production 2D					
Fine Model		Coarse Model (resolution 2x2)			
κ	q_{fine}	$\kappa_{eq,x}$	$\kappa_{eq,y}$	q_{coarse}	$E_p(\%)$
23,73	10,24	24,84	24,03	10,88	6%
0,09	0,53	0,10	0,09	0,68	27%
157,86	24,20	127,71	129,90	20,28	0%
50,83	21,02	57,61	58,80	22,14	5%
10,55	16,73	17,47	17,13	20,65	23%
323,22	25,00	215,55	214,29	25,14	0%

The results presented in Table 4 also show good agreement between fine and coarse scale, especially for high values of permeability. The results are only satisfactory when well is located in a region of low permeability ($\kappa \approx 10$).

SPE dataset 2-3D: the model is same described above, considering now three dimensions. The size simulates was 20x20x20 and its results are shown in Table 5.

Table 5. Results of production well flows, using the SPE's dataset number 2 in 3D.

SPE dataset 2 - Well Production 3D						
Fine Model		Coarse Model (resolution 2x2)				
κ	q_{fine}	$\kappa_{eq,x}$	$\kappa_{eq,y}$	$\kappa_{eq,z}$	q_{coarse}	$E_p(\%)$
36,90	70,10	38,77	58,36	44,98	92,45	31%
261,40	96,54	51,75	28,07	48,50	101,45	5%
3,47	36,85	1,50	0,05	5,47	36,41	1%
2487,8	104,23	295,75	5,08	12,61	105,78	1%
17,43	72,31	63,95	0,13	35,49	92,38	27%
119,16	89,14	38,77	58,36	44,98	92,61	3%

Observing the results in Table 5 it can be seen that the results are similar to the other cases, working well for high permeability locations and also for one single value low permeability location ($\kappa = 3{,}47$).

5 CONCLUSIONS

A novel technique for upcaling of absolute permeability was developed. The procedure is based on the conservation of flow rate for a given portion of the reservoir. The result is given by *D* equivalent permeability fields, where *D* is the Euclidean dimension. This also implies a generally anisotropic permeability field as an output.

The simulation time was decreased because of the size model reduction. The results in terms of production flow can be considered satisfactory, especially for well located in high permeability cells. Satisfactory results were registered in log-normal and SPE datasets. Most of the times, the simulation generates an important error when the production well is located in a low permeability block. However, for some particular cases, even if the permeability of the well-block is low the error is small.

It is left as suggestions for future works: i) the study of the number of rings must be done carefully: more rings will probably lead to a smaller influence of boundary conditions; ii) new models for wells located in low permeability blocks; iii) this numerical technique can also be improved and extended to more general cases such as multi-phase flows.

REFERENCES

Chen, Z., 2007. Reservoir Simulation: Mathematical Techniques in Oil Recovery, *Society for Industrial and Applied Mathematics*, Conference Series in Applied Mathematics.

Christie, M. A., 1996. Upscaling for Reservoir Simulation. *SPE, BP Exploration*.

Fitts, C. R., 2002. *Laminar and Turbulent Flow*, Groundwater Science, London, Academic press., Elsevier Science LTD, pp. 46-49.

Kruel-Romeu, R., 1994. *Écoulement en milieu hétéroène: prise de moyenne de perméabilite en régimes permanente et transitoire*}, PhD Thesis, Universitý of Paris VI/Paris, France.

Odsæter, L. V., 2013. Numerical Aspects of Flow Based Local Upscaling. Norwegian University of Science and Technology, Trondheim.

Renard, P., Marsily, G., 2000. Calculating equivalent permeability: A Review, *Water Resour. Res.*, vol. 20, pp. 261-262.

Skripkin, E., Kantzas, A. & Kryuchkov, S., 2014. Upscaling of reservoir properties, *GeoConvention focus 2014*.

Society of Petroleum Engineers- SPE Comparative Solution Project. http://www.spe.org/csp, 2001, also https://www.onepetro.org/journal-paper/SPE-72469-PA.

Warren, J.E., Price, H.H., 1961. Flow in heterogeneous porous media, *Society of Petroleum Engineering Journal*, vol. 1, pp.153-169.

Wen, X.H., Durlofsky, L.J., Edwards, M.G., 2003. Use of border regions for improved permeavility upscaling, *Mathematical Geology*, vol. 35, n 5, pp. 521-547.

Wen, X.H., Gómez-Hernández, J.J., 1996. Upscaling hydraulic conductivities in heterogeneous media: An overview, *Journal Hydrology*, vol. 183, n 1-2, pp.ix-xxxii.

White, C. D., Horne, R. N., 1987. Compting Absolute Transmissibility in the Presence of Fine-Scale Heterogeneity, *Society of Petroleum Engineering Journal, Ninth SPE Symposium on Reservoir Simulation*, Society of Petroleum Engineers, pp. 209-220.